

CONSTITUTIVE SOIL MODEL FOR EMBANKMENT OF RAILWAY FRAME BRIDGE

*Fang Dong¹, Erwin Oh¹, Ran An², Jialin Zhou³, Luhan Ma⁴ and Zhidao Sun⁵

¹ School of Engineering and Built Environment, Griffith University, Australia; ² Tong Yuan Design Group Co., Ltd, China; ³ Pier & Pile Consulting Engineers, Australia; ⁴ Wuhan Zhongtun Rail Transit Engineering Technology Co., Ltd, China; ⁵ Bridge Engineering Design and Research Institute, China Railway Engineering Design and Consulting Group Co., Ltd, China

*Corresponding Author, Received: 31 July 2024, Revised: 23 Oct. 2024, Accepted: 28 Oct. 2024

ABSTRACT: This paper examines the suitability of three different soil constitutive models to assess soil movement in the embankment of a railway bridge. As population and traffic demand continue to increase, the implementation of underpasses for roads beneath existing railways has emerged as a viable solution for enhancing current transport infrastructure. The section where the road intersects with railway tracks can be accommodated by constructing a frame bridge. From a stability perspective, the abutments are the crucial locations that may affect the operation of the railway. Numerical analysis is a crucial tool for examining the safety of projects by adopting an appropriate soil constitutive model. This paper analyses the characteristics of commonly used constitutive models for earth bodies. It combines this analysis with actual engineering cases to assess the applicability of these models during the construction of the transition section between the road and bridge on both sides of the railway jacking frame bridge. Considering the elasticity, the plasticity of the soil, and stress changes during actual loading and unloading conditions, three different constitutive models, namely, Mohr-Coulomb, modified Mohr-Coulomb, and HSS Model, are compared and analyzed using the finite element software Midas GTS NX. The results indicate that the HSS model provides numerical results similar to the field monitoring data. Considering that the numerical analysis results showed a similar trend with the field monitoring data, this study establishes a baseline for selecting the constitutive model for the bridge abutments on both sides of the top-in-frame bridge of the railway business line.

Keywords: Bridge abutment, Mohr-Coulomb, HSS model, Railway bridge embankment

1. INTRODUCTION

With the recent surge in large-scale infrastructure construction in China, the convergence of urban roads, municipal highways, and existing railways has become increasingly prevalent. This situation, bound by surrounding environmental conditions, necessitates controlling the additional settlement of the existing railway during the construction of new road projects within a limited range. This control is vital to prevent damage to the existing railway that could compromise the safety of railway operations.

Typically, when faced with such constraints, the preferred solution for road and railway crossings is the jacked frame bridge method. Integrating the railway line into the frame bridge offers advantages such as ease of construction, a simple structure, and minimal impact on the safety of existing railway transport during the construction process. Consequently, this approach is gaining popularity for the construction of frame bridges over existing railway lines.

To ensure that the impact of new road projects on the existing railway remains manageable, it is essential to conduct a safety assessment of the construction process during the design phase. The numerical results guide the implementation of

reasonable measures to mitigate the impact generated by the construction of the new road project. Central to this effort is the selection of the soil constitutive model, which is a key consideration in the design phase. The appropriate constitutive model accurately reflects real soil deformation and additional settlement.

However, it is observed that many structural engineers often underemphasize the study of geotechnical models. Instead, they frequently opt for the direct adoption of Mohr-Coulomb's constitutive model without systematically analyzing its influence on the additional settlement generated by adjacent existing structures.

However, new construction under diverse soil and loading conditions can result in varying effects on the stress level, stress path, stress history, and changes in the soil state of the existing ground. Alisawi conducted simulations of pile foundations behavior during earthquakes, utilizing three distinct soil constitutive models: Mohr-Coulomb, Drucker-Prager, and Cam-clay [1]. The study compared simulation results with experimental data from a physical shaking table, revealing that the Cam-Clay model closely matched the experimental outcomes. In contrast, the Mohr-Coulomb model failed to accurately represent the soil state when shear forces

exceeded the limit, often overestimating effective stress, leading to errors.

Furthermore, a modification of the Mohr-Coulomb model was proposed for the numerical analysis of pipeline engineering. The original model did not account for additional normal forces resulting from suction between soil particles. Adjusting the Mohr-Coulomb model allowed for a more accurate reflection of increased pipeline loads due to enhanced suction [2].

Ayman selected the Barcelona Basic Model as the soil constitutive model and used finite element software (Plaxis) to simulate issues related to settlement and uplift of shallow foundations on unsaturated soils [3]. Hejazi et al. employed three constitutive relationships—Mohr-Coulomb, Hardening soil model, and Hardening soil with small strain model—to simulate the construction of shallow tunnels. The results indicated that the Hardening soil model better-reflected volume strain and deviatoric strain caused by soil hardening [4].

Cettcto and Simonini analyzed the impact of granular flow on subsurface structures using Mohr-Coulomb and Drucker-Prager constitutive relationships [5]. They found that the elastic-plastic constitutive relationship responded more accurately at low shear rates, while the viscoplastic constitutive relationship was more appropriate at high shear rates. Ghadimi and Nikraz compared the effects of linear and nonlinear constitutive models in the numerical analysis of layered flexible pavements [6].

Chen et al. employed the Martin-seed-davidenkov viscoelastic model as a soil constitutive relationship to analyze the damage mechanism of subway structures in soft soils [7]. Brinkgreve integrated commonly used soil constitutive relations, such as Hooke's law, Mohr-Coulomb model, Drucker-Prager model, Duncan-Chang model, Cam-Clay model, Soft Soil model, and Hardening Soil model [8]. This integration enables geotechnical engineers to select appropriate soil constitutive models for foundation, tunnel, slope stability, and pit excavation projects.

In the case of the jacking frame bridge project, the primary influencing factor is the excavation of the pit beneath the existing railway foundation. The force analysis of the soil around the pit becomes intricate during the excavation and unloading process. Therefore, by comparing the settlement and deformation of the soil around the pit under different constitutive relationships, the one that closely approximates reality is selected for the analysis of the jacking frame bridge.

Zhang conducted a study on soil constitutive models and computational parameters through finite element numerical simulations of deep foundation pits [9]. Hu, utilizing field monitoring, theoretical analysis, and numerical simulations of a deep foundation pit project, concluded that the horizontal displacement of the deep foundation pit progressively

increases during the excavation process, with the maximum displacement occurring in the middle of the pit [10]. Song et al. employed the Hardening Soil Model for numerical analysis of foundation excavation. This model, considers the stress path correlation and compressive stiffness of soil deformation, reflecting changes in soil subjected to loading and unloading during construction [11]. Xue verified the reliability of the numerical analysis results for foundation excavation by comparing data from on-site monitoring with simulation results [12].

It is essential to study the applicability of soil constitutive relationships based on different construction conditions and locations. Baskari et al. studied how the strength and safety factor of volcanic clay in the Cililin area vary over time [13].

Despite these studies, the selection of a soil constitutive model for foundation excavation during the construction of a jacking frame bridge requires further investigation. Identifying a suitable constitutive model is crucial for accurately reflecting the real soil stress-strain relationship, which plays a significant role in predicting the risks associated with the jack-in frame bridge project.

In this paper, a three-dimensional finite element model of a railway jacking frame bridge, which includes the railway foundation, rails, sleepers, and other structural components, is established using the finite element analysis software MIDAS-GTS NX. The objective is to investigate the impact of three different soil constitutive models—specifically, the Mohr-Coulomb model, modified Mohr-Coulomb model (MMC model), and hardening soil with small strain model (HSS model)—on the existing railway foundation during the construction process under the jacking frame. The study aims to analyze which constitutive model's stress-strain relationship is more suitable for capturing the additional effects caused by the actual foundation excavation.

2. SOIL CONSTITUTIVE MODEL AND FINITE ELEMENT ANALYSIS

2.1 Mohr-Coulomb Material Model

The accuracy and convenience of the Mohr-Coulomb material model have contributed to its widespread adoption in geotechnical modeling.

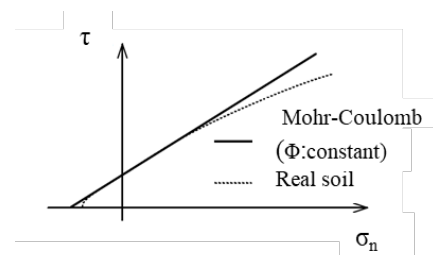


Fig.1 Mohr-coulomb yield guidelines [14]

The shear strength of the soil is presented in the following equation [15]:

$$\tau_f = c + \sigma \tan \varphi \quad (1)$$

where τ_f : shear stress, c : cohesion, σ : effective normal stress, and φ : the angle of shearing resistance.

In 1900, Mohr built upon Coulomb's earlier research and deduced that there is a single-valued functional relationship between the normal stress σ and the shear strength τ_f at the rupture surface of the soil, i.e.:

$$\tau_f = f(\sigma) \quad (2)$$

It is evident that the ultimate shear stress τ_f on any face is linked to the normal stress σ on that face. Soil failure occurs when the maximum Mohr circle is tangent to the Mohr-Coulomb yield envelope. Nevertheless, triaxial tests are conducted under the condition that $\sigma_2 = \sigma_3$, a circumstance rarely encountered in real-world situations. Further, soil failure occurs when the stress state is $\sigma_1 > \sigma_2 > \sigma_3$, and the Mohr-Coulomb yield criterion is applied.

$$\sigma_1 - \sigma_3 = -(\sigma_1 + \sigma_2) \sin \varphi + 2c \cos \varphi \quad (3)$$

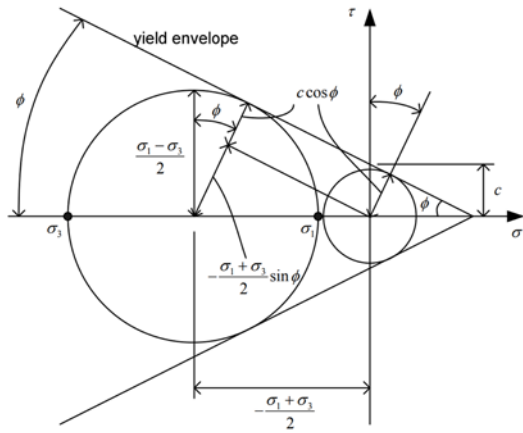


Fig.2 Geometric diagram of constitutive stress [14]

Equation (3) is established in terms of stress invariants in numerical simulations:

$$f(I_1, J_2, \theta) = -\frac{1}{3} I_1 \sin \varphi + \sqrt{J_2} \left(\cos \theta + \frac{1}{\sqrt{3}} \sin \theta \sin \varphi \right) - c \cos \varphi = 0 \quad (4)$$

where I_1 : the spherical tensor invariant, J_2 : the deviator tensor invariant, θ : the Lode angle.

2.2 Modified Mohr-Coulomb Material Model

The modified Mohr-Coulomb material model represents an enhanced extension of the traditional

Mohr-Coulomb model. In 1999, Schanz introduced the concept of soil hardening, where stress increment decreases with strain [16]. The modified Mohr-Coulomb model is fundamentally a material model that incorporates both nonlinear elasticity and plasticity. Its distinction from the Mohr-Coulomb model lies in defining the elastic zone as nonlinear elasticity, offering a more realistic representation.

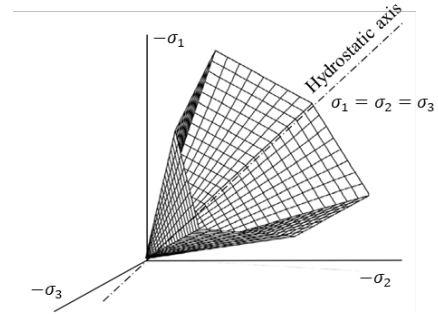


Fig.3 Mohr-Coulomb yield surface shape [14]

The yield criterion of the modified Mohr-Coulomb model is a decoupled double-hardening model, where shear and compressive failures do not affect each other. The expression of the double yielding function in the p-q plane is given by:

$$f_1 = \frac{q}{R_1(\theta)} - \frac{6 \sin \varphi}{3 - \sin \varphi} (p + \Delta p) = 0 \quad (5)$$

$$f_2 = (p + \Delta p)^2 + \alpha \left(\frac{q}{R_2(\theta)} \right)^2 - p_c^2 = 0 \quad (6)$$

where f_1 : shear yield function, f_2 : compression yield function, p : mean normal stress, q : generalized shear stress, p_c : hardening parameter.

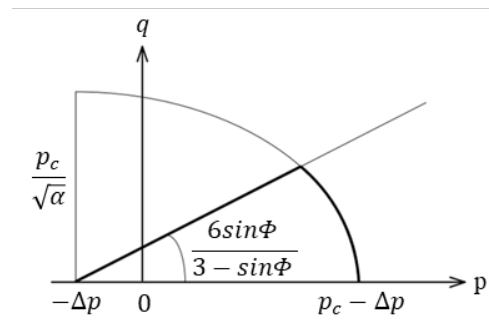


Fig.4 Yield function shape on p-q surface [14]

2.3 Hardening Soil With Small Strain Model

The Hardening Soil with Small Strain model (HSS) incorporates the increased stiffness of the soil at small strains, building upon the modified Mohr-Coulomb model. This adjustment is necessary because the hardened soil constitutive model assumes the soil's elasticity during both unloading and loading. Further, the soil does not exhibit linear elasticity or

elastically-ideally plastic behavior. The soil stiffness demonstrates nonlinearity as the strain range expands.

Specifically, the soil exhibits high stiffness at small strains, and as the strain increases, the soil stiffness decreases nonlinearly. The relationship between soil stiffness and strain follows an S-curve decay. In 1991, Atkinson defined three ranges of shear strains: very small strains (shear strains $< 10^{-6}$), small strains ($10^{-6} \leq$ shear strains $\leq 10^{-3}$), and large strains (shear strains $> 10^{-3}$) [17].

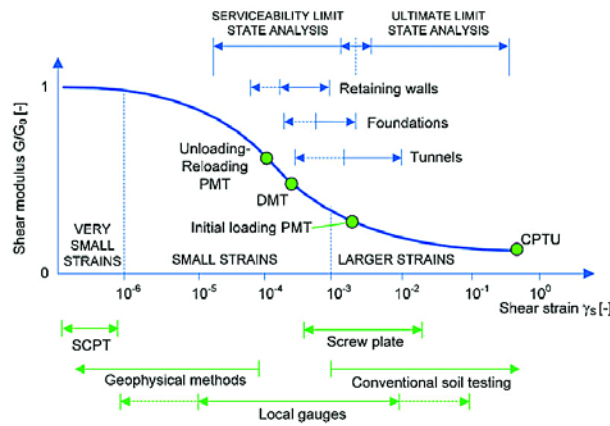


Fig.5 Soil stiffness-strain curve [18]

The HSS model considers similar soil parameters as the modified Mohr-Coulomb model, except that the HSS model adds two parameters for analyzing the HSS stiffness behavior, namely the initial HSS modulus G_0 and the shear strain level $\gamma_{0.7}$. Benz et al. proposed the overlay model in 2009, which takes into account the effects of average stress, pore ratio, and overconsolidation ratio [19]. In order to reflect these relationships, the HSS model uses the modified Hardin-Drnevich relationship equation to describe the soil stress-strain relationship curve in the HSS case.

$$\frac{G_s}{G_0} = \frac{1}{1+a \left| \frac{\gamma}{\gamma_{0.7}} \right|} , a = 0.385 \quad (7)$$

Where G_0 : initial shear modulus, G_s : shear modulus, γ : shear strain, $\gamma_{0.7}$: shear modulus, G_s decreases to the strain level of 70% G , a : constant.

2.4 Defining The Model

Using Midas GTS NX finite element analysis software, a three-dimensional model of the railway jacking frame bridge is established. The direction of the model and the analysis range are defined. Then, the X-axis of the model aligns with the existing railway direction, the Y-axis is oriented vertically to the existing railway direction and represents the jacking frame bridge direction, and the Z-axis represents the direction of gravity. Considering the possible influence range specified in the technical

specifications of urban rail transit engineering monitoring, which is 2~3 times the excavation depth, the analysis range is determined [20]. To include this influence range, the model dimensions are set at 70 m in the X-axis direction, 70 m in the Y-axis direction, and 25 m in the Z-axis direction. The Finite Element model of the railway frame bridge is illustrated in Figure 6.

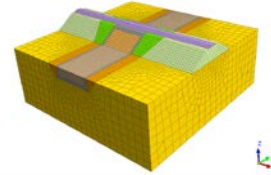


Fig.6 Railway topping frame bridge model and analysis scope

2.5 Defining The Model

In this paper, the finite element software MIDAS-GTS NX is adopted with the following assumptions:

1. The soil in the model is assumed to be homogeneous and isotropic.
2. The elastic properties based on Hooke's law are selected for the steel rails, sleepers, jacked frame bridges, transition section backfill materials, and the soils parameters [21-29].
3. Interfaces are set up between the rails, sleepers and ballast for analysis [27].
4. The influence of groundwater is not considered.
5. The effect of seismic activity is not considered.

2.6 Computational Models

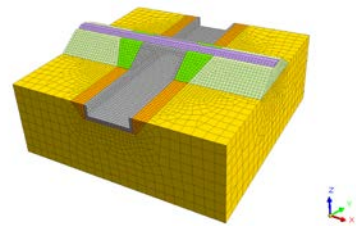


Fig.7 Illustrative model of railway with frame bridge

The modelling sequence involves several steps: (a) one-dimensional unit components such as the existing railway track and sleepers are established; (b) three-dimensional solid units are created in a sequence from smaller to larger components; (c) boundary conditions are set, loads are applied to the model; (d) the model is simulated under construction stages. The model components include:

1. Three-dimensional units: In addition to the rails and sleepers simulated using the 1D beam unit, other structural components are represented by three-dimensional solid units in the simulation. These include soil, ballast, subgrade, frame bridge, and transition section. The model utilizes a six-node

tetrahedral unit for these components, as the displacement and stress results produced by this modelling approach closely approximate the actual conditions. The details of the model's structural components are illustrated in Figure 8.

2. Boundary Conditions: boundary conditions, also referred to as stress analysis boundaries, are typically artificial conditions used in static analysis. They serve the purpose of simulating the constraint effect of the surrounding strata in each direction within the analysis area selected by the model.

3. Applied load: Gravity loads are applied across the entire model to simulate the effects of gravitational forces. Train loads are imposed on the rails to account for the weight and forces associated with trains, while highway vehicle loads are applied to the frame bridge deck to simulate the impact of vehicles on the structure. These load applications help capture the dynamic responses and stresses induced by the various loads that the jacking frame bridge may experience in real-world conditions.

4. Setting the construction conditions: Given that the model is specifically designed to analyze the transition section of a railway into a frame bridge and focuses primarily on the static effects of the constitutive relationships of different transition sections, the analysis does not include the entire process of jacking the frame bridge to examine its operating condition. Instead, a comparison is made between the original state and the state after jacking the frame bridge to assess the effects of different constitutive relationships on the transition segment.

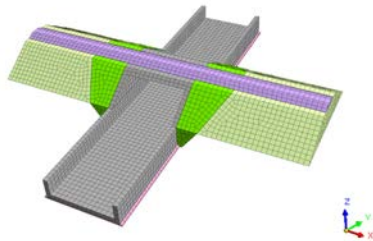


Fig.8 Model of structural components

3. RESULTS AND ANALYSIS

3.1 Settlement And X-Direction Displacement Analysis of The Transition Section

The results are presented with capturing output contour images from the software. The images (see Figures 9 to 15) are captured from a selected cross section of the model. Figure 9 provides the cross sections to be analysed, where cross sections a-a and b-b are used to determine the horizontal displacement, and cross section c-c is to determine the vertical displacement. There are some on-site monitoring points named A, B, C, and D. The maximum settlement in the view of cc section is -8.09763 mm under the

Mohr-Coulomb model, -3.28191 mm under the modified Mohr-Coulomb model, and -3.26045 mm under the HSS model.

For the analysis of horizontal displacement variation, the horizontal displacement along the direction of the railway line (horizontal displacement in the X-axis direction) is selected. The maximum horizontal displacements of sections aa and bb are 1.89706 mm and -1.89392 mm, respectively, under the Mohr-Coulomb model. Under the modified Mohr-Coulomb model, the case of the small strain model, the maximum horizontal displacements of sections aa and bb are 0.625812 mm and -0.611103 mm, respectively. The horizontal displacement perpendicular to the direction of the railway right-of-way (Y-axis direction) exhibits minimal changes and will not be discussed in this paper.

Figures 10, 11, and 12 depict the settlement (induced by the installation of the frame bridge and the removal of soil) in the transition area when the Mohr-Coulomb model, the modified Mohr-Coulomb model, and the HSS model are successively selected for the jacking frame bridge.

The calculation results clearly indicate that the HSS model is the soil constitutive model that causes the least settlement in the transition section during the construction of the jack-in frame bridge. The settlement in the transition section near the jack-in frame bridge side is -0.9581 mm and -0.9688 mm, while the settlement in the transition section near the existing subgrade side is -0.9726 mm and -0.9971 mm, respectively.

In comparison, the settlement in the transition section is slightly higher when the modified Mohr-Coulomb model is used. The settlement near the jacked frame bridge side is -1.0064 mm and -1.001 mm, while the settlement near the existing subgrade side is -1.0092 mm and -1.0112 mm, respectively.

However, when the Mohr-Coulomb model is chosen as the soil constitutive model. The additional settlement in the transition section due to the construction of the jack-in frame bridge is 5 to 6 times greater than that of the first two models. Specifically, the settlement of the transition section near the top-in frame bridge side is -5.6979 mm and -5.7047 mm, while the settlement of the transition section near the existing subgrade side is -5.6555 mm and -5.6600 mm, respectively.

In terms of the change in displacement in the x-axis direction, the HSS model exhibits the smallest values, followed by the Modified Mohr-Coulomb model for the additional horizontal displacement in the transition section on the side close to the framed bridge. The largest values were -0.056 mm and 0.0012 mm, 0.0063 mm and -0.0061, 0.0245 mm and -0.0238 mm, respectively.

However, the transition section on the side close to the established subgrade presented the opposite situation. The Mohr-Coulomb model showed the smallest change in displacement along the x-direction, followed by the Modified Mohr-Coulomb model, and the small strain model showed the largest change in displacement along the x-direction. Their magnitudes

are 0.007 mm and -0.0088 mm, -0.0245 mm and 0.0226 mm, -0.424 mm and 0.0357 mm, respectively.

Overall, the construction of the jacked frame bridge has less impact on the transition section along the alignment direction, and the focus of attention should be on the vertical settlement.

Table 1. Soil layer parameters

Soil	Soil depth m	Unit weight kN/m ³	Friction angle °	Cohesion kN/m ²	Deformation modulus MPa	Bearing capacity KPa	Poisson ration	Thermal expansivity	Damping ratio
Silty Clay	25	19	13.8	21.8	11	70	0.3	1×10 ⁻⁶	5%

Table 2. Structural member parameters (elastic constitutive structure)

Structural member	Unit weight / (KN/m ³)	Elasticity modulus / (MPa)	Poisson ration	Thermal expansivity	Damping ratio
Rail	78.5	2.1×10 ⁵	0.3	1.25×10 ⁻⁵	5%
Railway ballast	21	2.4×10 ²	0.36	1.25×10 ⁻⁵	5%
Subgrade	18	30	0.2	1.2×10 ⁻⁵	5%
Jacking frame bridge	25	3.4×10 ⁴	0.2	1.2×10 ⁻⁵	5%
Fill back in transition section	23.6	3.0×10 ⁴	0.2	1.2×10 ⁻⁵	5%

Table3. Finite element analysis working conditions

NO.	Phase	Phase content
1	Initial stress state of soil layer	Activate the soil, add the dead weight and boundary conditions, and clear the dead weight displacement of soil
2	Status of existing railway line	Activate existing subgrade, track and corresponding load
3	Displacement zeroing	Clear the displacement of structure and soil
4	Jacking in frame bridge	Passivating excavation soil, activating frame bridge, adding highway vehicle load

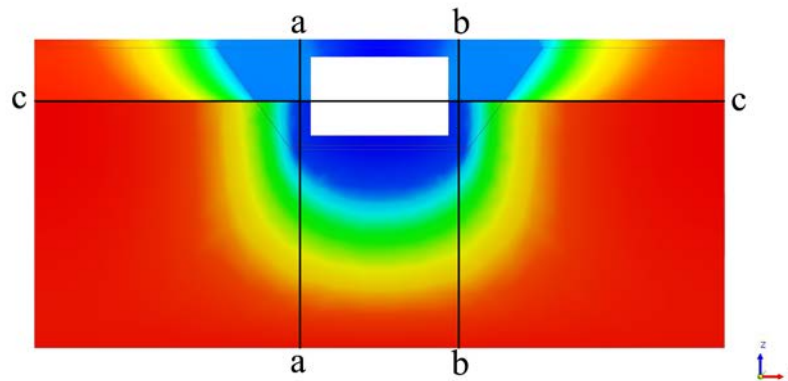


Fig.9 Illustrative cross-sections and on-site monitoring points for analysis

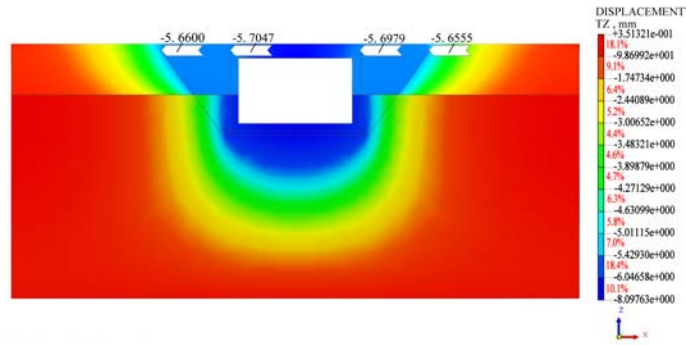


Fig.10 Settlement diagram for the transition section under the Mohr-Coulomb constitutive model (unit: mm)
 NOTE: To reflect in Text. The figure is captured from “y” direction (refer to Figure 7).
 Uniform Load of 37.36 kN/m² is applied on the track elements [30].

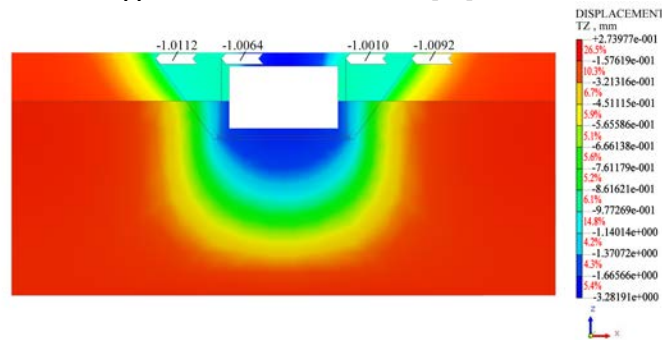


Fig.11 Settlement diagram generated to the transition section under the modified Mohr-Coulomb constitutive model (unit: mm)

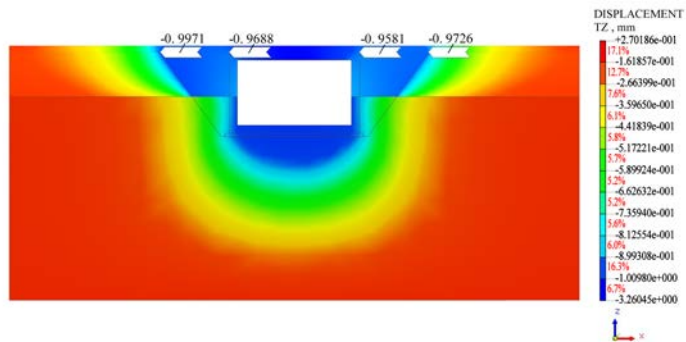


Fig.12 Settlement diagram for the transition section under the HSS constitutive model (unit: mm)

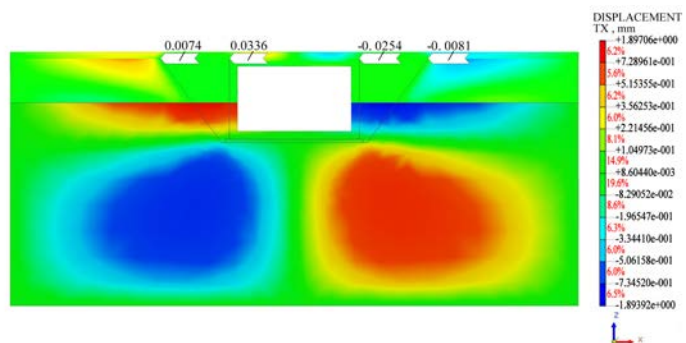


Fig.13 Horizontal displacement (x direction) diagram for the transition section under the Mohr-Coulomb constitutive model (unit: mm)

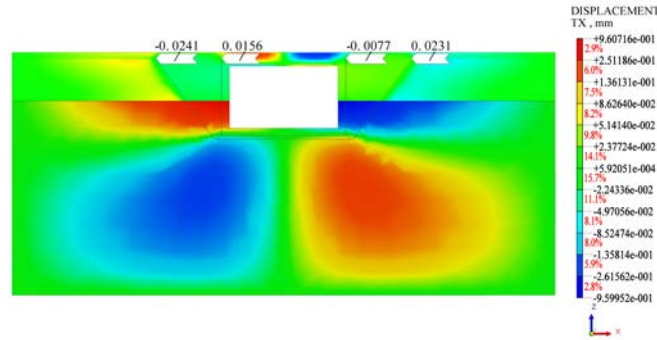


Fig.14 Horizontal displacement (x direction) diagram for the transition section under the modified Mohr-Coulomb constitutive model (unit: mm)

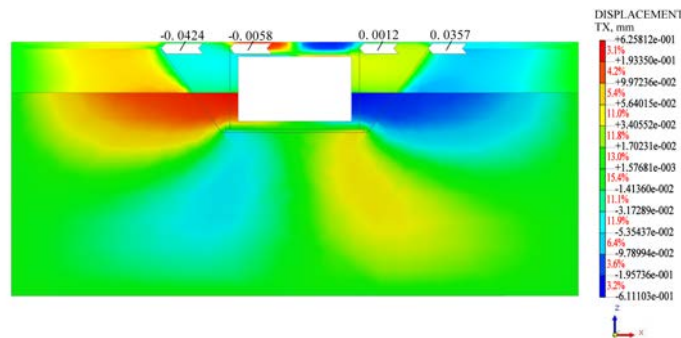


Fig.15 Horizontal displacement (x direction) diagram for the transition section under the HSS constitutive model (unit: mm)

Through the comparative analysis of the additional settlement mentioned above, it can be concluded that the magnitude of settlement varies for different soil constitutive models. Therefore, selecting the proper constitutive model for the project according to different engineering requirements is extremely necessary. Additionally, the commonly used Mohr-Coulomb model may not be applicable because the construction process of jacked frame bridges involves a large range of foundation excavation. The main reason is that the Mohr-Coulomb model is more suitable for projects with unilateral loading, and the process of unloading and reloading cannot be accurately calculated. In contrast, the modified Mohr-Coulomb model and the HSS model exhibit relatively similar settlement magnitudes. This aligns with the calculation principles of the two material models, except that the small-strain model takes into account the change in stiffness of the soil in the small-strain state. The maximum settlements and maximum horizontal displacements regarding sections aa, bb, and cc are organized in Table 4 and Table 5.

Table 4. Summary of maximum settlement

Model	Maximum settlement(mm)
Mohr-Coulomb	-8.098
MMC	-3.282
HSS	-3.261

Table 5. Summary of maximum horizontal displacement

Model	Maximum horizontal displacement(mm)	
	a-a	b-b
Mohr-Coulomb	1.89706	-1.89392
MMC	0.960716	-0.959952
HSS	0.625812	-0.611103

3.2 Comparison of Numerical Analysis Results With On-Site Monitoring Results

To validate the effectiveness of the numerical analysis results, a comparison is made with the on-site monitoring vertical deformation results of a top-in frame bridge under an existing railway subgrade at a location in Shandong. The backfill material for the transition section in the site project is C25 concrete, and the soil in the bearing layer is powder clay. Therefore, this paper specifically compares the transition section on both sides of the top-in frame bridge of the railway business line in the case of powder clay in the bearing layer.

According to actual monitoring experience, once the backfilling of the transition section is completed, the beams are dismantled. In cases where construction activities within the railway line are minimal, the use of a static level automated settlement monitoring system, while ensuring accuracy, allows

for a high monitoring frequency. This facilitates 24-hour real-time online monitoring, enabling a prompt response to dynamic changes in the settlement of newly built bridges, culverts, the transition section, and the existing subgrade.

The system comprises a liquid storage tank, base point, measuring point, collection equipment, and data transmission equipment. The static level meter includes the main container, connecting pipe, sensor, and other components. The static level meter employs the principle of connecting liquid for settlement observation, where multiple connecting tubes maintain a consistent liquid surface level. By measuring the liquid height of various storage tanks and performing calculations, the relative difference in height values for each static level meter can be derived.

Once the monitoring data collected by the on-site collection terminal enters the processing server, the data processing software parses the data. The data analysis and display function then facilitate the monitoring of deformation statistics and evaluation, issuing warnings as needed.

Simultaneously, the processed data and interpreted results are stored in the database. The database, containing historical monitoring data and information on early warning, time, and health status, provides essential data for the analysis module and other purposes.

The system collects data through wired cables, transmitting it to the monitoring center server via a wireless GPRS transmitter. After processing, the system outputs the monitoring physical quantities and transmits the data through the network.

The monitoring period for the entire project spanned 425 days, with an additional year of monitoring following project completion. The site comparison data used in this paper are from the last day of monitoring

In Fig. 16, the blue points represent the settlement result of numerical analysis when using Mohr-Coulomb as the soil constitutive model, the red points are the settlement result of numerical analysis when modifying Mohr-Coulomb as the soil constitutive model, the grey points are the settlement result of numerical analysis when the HSS model is the soil constitutive model, and the yellow points are the settlement result of monitoring in the actual field project. In the figure, only four nodes are selected for comparison, which are the two points near the frame bridge and the two points near the existing subgrade in the transition section on both sides.

The evident result from the figure is that when the soil adopts the HSS and modified Mohr-Coulomb constitutive model, the additional settlement generated in the transition section is only slightly larger than the actual field monitoring data, approximately 1.2 times. However, the additional settlement generated when the Mohr-Coulomb

constitutive model of the soil is used is 6-7 times greater than the settlement data monitored in the field.

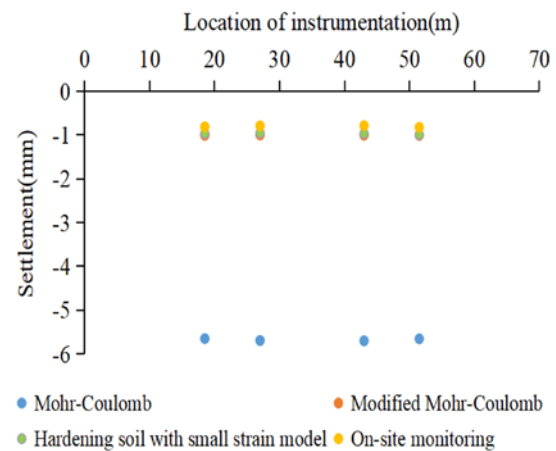


Fig.16 Numerical analysis of settlement compared with settlement from field monitoring (unit: mm)

As shown in the calculation results, it is concluded that the Mohr-Coulomb model is not the best model to analyse the construction of the jacked-in frame bridge, and the modified Mohr-Coulomb and HSS models can reflect the settlement behavior of such projects more accurately. Typically, during the actual construction process, the construction company will conduct foundation treatment and protective measures at the jacked-in frame bridge, causing the field monitoring results to be smaller than the numerical analysis results.

Further, the numerical results are larger than the actual soil is because the parameters of the numerical analysis are adopted from the triaxial test, which assumes that the second constitutive stress is equal to the minimum constitutive stress (see Table 1). However, in the actual situation, the second constitutive stress is usually greater than the minimum constitutive stress, making the soil properties better. The trend and range of the monitoring results can match well with the calculated results of numerical analysis, verifying the reliability of the numerical calculation model in this paper. Based on the accuracy verification of the numerical solution and the real solution, it is reasonable to assume that the numerical model calculation results also have good credibility to a certain extent.

In summary, the process of topping the railway business line into the frame bridge involves excavation of the pit, soil unloading, and differences in road and bridge structure stiffness, which can result in additional settlement. The establishment of the transition section is crucial to mitigate the impact of additional settlement and ensure a more accurate prediction of the additional settlement caused by the transition section through numerical analysis. The numerical analysis results are then compared with

field monitoring results. It is verified that the Mohr-Coulomb model is not suitable for this type of project, and additional parameters need to be considered for the correction. Both the modified Mohr-Coulomb and HSS models are found to be suitable for this type of project, with the HSS model showing the closest match to the actual situation when compared with field monitoring data. For the construction of the jacking frame bridge, the following recommendations are made:

1. Strengthen the protection of the foundation pit before initiating the jacking frame bridge construction. Monitor the displacement of the foundation and the surrounding soil closely during the excavation process. Implement timely countermeasures if any abnormal deformation is observed.

2. Ensure meticulous execution of the construction steps during the jacking frame bridge construction, including overhead work, excavation, bottom clearing, measurement, jacking, and repetitive jacking. Regularly monitor and measure throughout the construction process to ensure accuracy and address any issues promptly.

In addressing common jacking construction problems, such as scheduled immobility, back damage, jacking bias, or low lifting, it is essential to promptly identify the causes and implement rapid processing to avoid potential dangers. Swift and effective actions can prevent further complications and ensure the safety and success of the jacking construction project.

4. CONCLUSION

Based on the finite element method, a three-dimensional numerical calculation of the transition section of a railway business line jacking frame bridge was conducted, and the model's accuracy was verified by comparing it with field monitoring results. The following conclusions were drawn:

1. For the construction of top-in frame bridges, it is recommended to use the modified Mohr-Coulomb model or HSS model as the soil model.

2. The numerical analysis with HSS model and modified Mohr-Coulomb model showed similar trends with the field monitoring data. This suggests that the second constitutive stress in actual soil plays a more significant role than assumed in laboratory triaxial tests, where it is equal to the third constitutive stress. The numerical analysis does not fully represent the actual corrective measures implemented during construction. Further research, especially on the parameters of the modified Mohr-Coulomb model and the HSS model, is necessary.

The research results can serve as a reference for selecting the soil model for the transition section of the railway line jack-in frame bridge.

5. REFERENCES

- [1] Alisawi A.T., P. E. F. Collins, and K. A. Cashell., Nonlinear Numerical Simulation of Physical Shaking Table Test, Using Three Different Soil Constitutive Models. *Soil Dynamics and Earthquake Engineering*, Vol. 143, 2021, 106617.
- [2] Robert D. J., A Modified Mohr-Coulomb Model to Simulate the Behavior of Pipelines in Unsaturated Soils. *Computers and Geotechnics*, Vol. 91, 2017, pp. 146-160.
- [3] Abed A.A. and Vermeer P.A., Numerical Simulation of Unsaturated Soil Behaviour. *International journal of computer applications in technology*, Vol. 34, Issue 1, 2009, pp.2-12.
- [4] Hejazi Y., Dias D., and Kastner R., Impact of Constitutive Models on the Numerical Analysis of Underground Constructions. *Acta Geotechnica*, Vol. 3, 2008, pp. 251-258.
- [5] Ceccato F., and Simonini P., Granular Flow Impact Forces on Protection Structures: MPM Numerical Simulations with Different Constitutive Models. *Procedia Engineering*, Vol. 158, 2016, pp.164-169.
- [6] Ghadimi B., and Nikraz H., A Comparison of Implementation of Linear and Nonlinear Constitutive Models in Numerical Analysis of Layered Flexible Pavement. *Road Materials and Pavement Design*, Vol. 18, Issue 3, 2017, pp. 550-572.
- [7] Guoxing C., Su C., Xi Z., Xiuli D., Chengzhi Q. I., and Zhihua, W., Shaking-table Tests and Numerical Simulations on a Subway Structure in Soft Soil. *Soil Dynamics and Earthquake Engineering*, Vol. 76, 2015, pp. 13-28.
- [8] Brinkgreve R.B., For Chapter in a Book, Selection of soil models and parameters for geotechnical engineering application. In *Soil constitutive models: Evaluation, selection, and calibration*, 2005, pp. 69-98.
- [9] Zhang, C.H., Studies on Pit Excavation Numerical Simulation and Soil Constitutive Model and Parameter Back-analysis (Doctoral dissertation, Ocean University of China). 2007, (in Chinese).
- [10] Hu, N. Numerical Simulation of a Deep Foundation Pit of the Underground Plaza in Hefei and Inverse Analysis of Parameters (Master dissertation, Hefei University of Technology). 2013, (in Chinese).
- [11] Song, G. and Song, E.X., Selection of Soil Constitutive Models for Numerical Simulation of Foundation Pit Excavation. *Engineering Mechanics*, Vol. 05, 2014, pp.86-94. (in Chinese).
- [12] Xue, F., Design, Monitoring and Numerical Simulation of a Deep Foundation Pit Support Project in Shanghai (Master dissertation, Tianjin University). 2013, (in Chinese).

- [13] Baskari T., Zakaria Z., Sulaksana, N. and Muljana, B., Study on Rheological Constitutive Model of Cililin Volcanic Clay, Indonesian Relation to Long-Term Slope Stability. *International Journal of GEOMATE*, Vol. 21, Issue 86, 2021, pp.40-47.
- [14] MIDAS-GTS, User's Manual. Beijing Midas Technology Co., Ltd, 2004.
- [15] Craig, R. F., *Craig's Soil Mechanics*. CRC Press, 2004, pp.1-570
- [16] Schanz T., Vermeer P. A., and Bonnier P. G., The Hardening Soil Model: Formulation and Verification. *Beyond 2000 in Computational Geotechnics*, Vol. 1, 1999, pp. 281-296.
- [17] Atkinson, J. H., Experimental Determination of Stress-strain-time Characteristics in Laboratory and In-situ Tests. General Report. In Proc. 10th Eur. Conf. Soil Mech. and Fnd Engng Vol. 3, 1991, pp. 915-956.
- [18] Truty A., Obrzud, and R. Komputerowa Computer Analysis of Interaction between Structures under Construction and the Subsoil Using Advanced Models of Constitutive Soils, Calibrated Based on Laboratory and Field Test Results. In *Proceedings of the 27th Polish Workshops for Structural Designers*, 2013. (in Polish)
- [19] Benz, T., Vermeer, P. A., and Schwab, R., A Small-strain Overlay Model. *International Journal for Numerical and Analytical Methods in Geomechanics*, Vol. 33, Issue 1, 2009, pp. 25-44.
- [20] Zhang R.J., and Hu Q.F., Comparative Analysis of Finite Element Simulation Results for Mohr-Coulomb and Modified Mohr-Coulomb Intrinsic. *China Real Estate Industry*, Vol. 08, 2 015, pp. 256-258. (in Chinese).
- [21] Sun L. and Zhao N., Finite Element Analysis of the Effect of Deep Foundation Excavation on the Displacement of Adjacent Railroad by Different Soil Principal Models. *China Water Transportation*, Vol. 21, Issue 10: 2021, pp. 119-121. (in Chinese).
- [22] Jiang M.J, Zhu F.Y. and Liu F., Applicability of Two Constitutive Models to Numerical Simulation of Foundation Excavation. *Journal of Hohai University (Natural sciences)*, Vol. 40 Issue 05, 2012 pp. 568-575. (in Chinese).
- [23] Jiang, J. H. T., and Cui, J. Y., Analysis of the Effect of Different Soil Constitutive Models on the Numerical Simulation Results of Pit Excavation. *Chinese Journal of Construction Technology*, 2011. (in Chinese).
- [24] Li G.X., Some Problems in Researches on Constitutive Model of Soil. *Chinese Journal of Geotechnical Engineering*, Vol. 31, Issue10, 2009, pp. 1636-1641. (in Chinese).
- [25] Zhang J.X., Zhao G., Zhang L., and Jiang H., Application of HSS Model in Shield Simulation and Parameter Sensitivity Research. *Chinese Journal of Underground Space and Engineering*, Vol. 16, Issue S2, 2020, pp. 618-625. (in Chinese).
- [26] Committee for the Preparation of the Engineering Geology Handbook. *China Construction Industry Press*, 2018. (in Chinese).
- [27] Sheng, X.Y., MC, HS, HSS Constitutive Models Adopted in Comparative Analysis of Deep Excavation Modelling. *Low Temperature Architecture Technology*, 2020, (in Chinese).
- [28] Luo, M.M, Chen Y., and Zhou, J., Research Status and Prospect of Parameter Selection for the HS-Small Model. *Industrial Construction*, Vol. 51, Issue 04, 2021, pp. 172-180. (in Chinese).
- [29] Zhang H., Zhang C.R, Shi Z.H., Numerical Simulation of Excavation Effects on Tunneling with IGS Small Strain Model. *Chinese Journal of Geotechnical Engineering*, Vol. 43, Issue S2, 2021, pp. 72-75.
- [30] Code for design of railway earth structure. *Industry Standards of the People's Republic of China*, 2016, pp.1-234. (in Chinese).

Copyright © Int. J. of GEOMATE All rights reserved, including making copies, unless permission is obtained from the copyright proprietors.
